NeuroImage 289 (2024) 120537

Contents lists available at ScienceDirect

NeuroImage

journal homepage: www.elsevier.com/locate/ynimg

Technical Note

Partial volume correction in longitudinal tau PET studies: is it really needed?

Alejandro Costoya-Sánchez [a,b,1], Alexis Moscoso [c,d,1], Tomás Sobrino [e,f], Álvaro Ruibal [a,b], Michel J. Grothe [c,d,f,g], Michael Schöll [c,d,h], Jesús Silva-Rodríguez [f,g,*], Pablo Aguiar [a,b,f,*], for the Alzheimer's Disease Neuroimaging Initiative[2]

[a] Molecular Imaging Group. Center for Research in Molecular Medicine and Chronic Diseases (CIMUS), University of Santiago de Compostela (USC), Campus Vida, Santiago de Compostela, Av. Barcelona SN, 15782, Santiago de Compostela, Galicia, Spain
[b] Nuclear Medicine Department and Molecular Imaging Group, Instituto de Investigación Sanitaria de Santiago de Compostela, Travesía da Choupana s/n, Santiago de Compostela, Spain
[c] Wallenberg Centre for Molecular and Translational Medicine, University of Gothenburg, Gothenburg, Sweden
[d] Department of Psychiatry and Neurochemistry, Institute of Physiology and Neuroscience, University of Gothenburg, Gothenburg, Sweden
[e] NeuroAging Laboratory Group (NEURAL), Clinical Neurosciences Research Laboratories (LINC), Health Research Institute of Santiago de Compostela (IDIS), University Clinical Hospital, Santiago de Compostela, Spain
[f] Centro de Investigación Biomédica en Red sobre Enfermedades Neurodegenerativas, Instituto de Salud Carlos III, Madrid, Spain
[g] Reina Sofía Alzheimer's Centre, CIEN Foundation, ISCIII, Madrid, 28031, Spain
[h] Dementia Research Centre, Institute of Neurology, University College London, London, United Kingdom

ARTICLE INFO

Keywords:
Tau PET
PVC
Longitudinal
Off-target binding, SUVR

ABSTRACT

Background: [^{18}F]flortaucipir (FTP) tau PET quantification is known to be affected by non-specific binding in off-target regions. Although partial volume correction (PVC) techniques partially account for this effect, their inclusion may also introduce noise and variability into the quantification process. While the impact of these effects has been studied in cross-sectional designs, the benefits and drawbacks of PVC on longitudinal FTP studies is still under scrutiny. The aim of this work was to study the performance of the most common PVC techniques for longitudinal FTP imaging.

Methods: A cohort of 247 individuals from the Alzheimer's Disease Neuroimaging Initiative with concurrent baseline FTP-PET, amyloid-beta (Aβ) PET and structural MRI, as well as with follow-up FTP-PET and MRI were included in the study. FTP-PET scans were corrected for partial volume effects using Meltzer's, a simple and popular analytical PVC, and both the region-based voxel-wise (RBV) and the iterative Yang (iY) corrections. FTP SUVR values and their longitudinal rates of change were calculated for regions of interest (ROI) corresponding to Braak Areas I-VI, for a temporal meta-ROI and for regions typically displaying off-target FTP binding (caudate, putamen, pallidum, thalamus, choroid plexus, hemispheric white matter, cerebellar white matter, and cerebrospinal fluid). The longitudinal correlation between binding in off-target and target ROIs was analysed for the different PVCs. Additionally, group differences in longitudinal FTP SUVR rates of change between Aβ-negative (A-) and Aβ-positive (A+), and between cognitively unimpaired (CU) and cognitively impaired (CI) individuals, were studied. Finally, we compared the ability of different partial-volume-corrected baseline FTP SUVRs to predict longitudinal brain atrophy and cognitive decline.

Results: Among off-target ROIs, hemispheric white matter showed the highest correlation with longitudinal FTP SUVR rates from cortical target ROIs (R^2=0.28–0.82), with CSF coming in second (R^2=0.28–0.42). Application of voxel-wise PVC techniques minimized this correlation, with RBV performing best (R^2=0.00–0.07 for hemispheric white matter). PVC also increased group differences between CU and CI individuals in FTP SUVR rates of change across all target regions, with RBV again performing best (No PVC: Cohen's d = 0.26–0.66; RBV: Cohen's d =

* Corresponding authors.
E-mail addresses: jsilva@fundacioncien.es (J. Silva-Rodríguez), pablo.aguiar@usc.gal (P. Aguiar).

[1] Equally contributing authors

[2] Data used in the preparation of this article were obtained from the Alzheimer's Disease Neuroimaging Initiative (ADNI) database (adni.loni.usc.edu). As such, the investigators within the ADNI contributed to the design and implementation of ADNI and/or provided data but did not participate in the analysis or the writing of this report. A complete listing of ADNI investigators can be found at: http://adni.loni.usc.edu/wpcontent/uploads/how_to_apply/ADNI_Acknowledgement_List.pdf

https://doi.org/10.1016/j.neuroimage.2024.120537
Received 12 December 2023; Received in revised form 7 February 2024; Accepted 8 February 2024
Available online 15 February 2024

0.43–0.74). These improvements were not observed for differentiating A- from A+ groups. Additionally, voxel-wise PVC techniques strengthened the correlation between baseline FTP SUVR and longitudinal grey matter atrophy and cognitive decline.
Conclusion: Quantification of longitudinal FTP SUVR rates of change is affected by signal from off-target regions, especially the hemispheric white matter and the CSF. Voxel-wise PVC techniques significantly reduce this effect. PVC provided a significant but modest benefit for tasks involving the measurement of group-level longitudinal differences. These findings are particularly relevant for the estimations of sample sizes and analysis methodologies of longitudinal group studies.

1. Background

Over the recent years, positron emission tomography (PET) has become the reference tool for the *in vivo* evaluation of amyloid-beta (Aβ) plaques and tau neurofibrillary tangles in Alzheimer's Disease (AD) (Schöll et al., 2016; Schultz et al., 2018). Among the wide range of tau PET radiotracers available (Gogola et al., 2022; Lemoine et al., 2017), [^{18}F]flortaucipir (FTP) has been the most studied, demonstrating its ability for the *in vivo* detection and monitoring of AD-related 3R/4R tauopathy (Chien et al., 2013; Leuzy et al., 2019). Both *post-mortem* and *in-vivo* studies have demonstrated that FTP-PET is able to stage AD tauopathy based on the quantification of FTP standardized uptake value ratios (SUVR) within regions of interest (ROIs) representing the different Braak areas (Schöll et al., 2016; Soleimani-Meigooni et al., 2020). During the last decade, FTP has become an essential tool for AD research and clinical trials of disease-modifying drugs (Ossenkoppele et al., 2021; Teng et al., 2022), and its recent approval by the FDA may result on an increasing use of the tracer in the clinic.

Despite recent advancements on its applications, FTP-PET is still hampered by technical limitations inherent to PET imaging, such as noise and limited spatial resolution. Specifically, FTP-PET has been notorious for showing unspecific uptake in non-cortical areas such as the white matter, the basal ganglia and, the choroid plexus, among others (Baker et al., 2019; López-González et al., 2022), which degrades image quantification via partial volume effects (PVE). The unspecific uptake in these off-target ROIs results in a "spill-in" effect into neighbouring regions, causing an overestimation of the true activity levels, or, in the case of tau PET, and overestimation of the tau accumulation (Aston et al., 2002; Lu et al., 2021). Furthermore, a complementary spill-out effect in the opposite direction can also occur, making activity from small regions with high activity, such as the hippocampus or the entorhinal cortex, "spill-out" to adjacent regions. While novel (usually named "second generation") tau PET tracers have significantly reduced off-target binding (Bischof et al., 2021), PVE is still considered to play an important role in longitudinal studies, as it increases with cortical thinning. To mitigate these effects, several Partial Volume Correction (PVC) techniques have been developed over the years (Erlandsson et al., 2012). Previous work from our group and others has demonstrated that PVC methods provide a significant benefit for FTP-PET quantification in cross-sectional studies, at least at the group level (Baker et al., 2019; López-González et al., 2022). However, even though PVCs are effective for removing *spill-in* and *spill-out* counts in FTP-PET, they usually result in significant image degradation in the form of increased noise and artifacts, increasing the variability of cortical SUVRs (Erlandsson et al., 2012). This increased variability could severely penalize the ability of tau PET to measure small variations in tau accumulation over time. While several tau PET longitudinal studies have already incorporated PVC in the pipeline analysis, the impact and expected benefit of PVC on longitudinal studies is still under discussion (Schwarz et al., 2021) . Thus, in the present work we aimed at carrying out a systematic evaluation of the performance of different PVC techniques in common longitudinal FTP-PET metrics. To this end, we evaluated the impact of off-target binding on the ability of FTP-PET to assess longitudinal changes in FTP SUVRs. Additionally, we studied whether PVC increases FTP SUVR differences between groups that are well-known for showing diverging trajectories of tau accumulation, such as between Aβ PET negative (A-) and positive (A+) participants, as well as between cognitively unimpaired (CU) and cognitively impaired (CI) individuals (Jack et al., 2018). Finally, we studied the impact of PVC on the performance of baseline FTP SUVRS to predict longitudinal atrophy and cognitive decline.

2. Methods

2.1. Participants

The data used in the preparation of this article were obtained from the Alzheimer's Disease Neuroimaging Initiative (ADNI) database. The ADNI was launched in 2003 as a public-private partnership, led by Principal Investigator Michael W. Weiner, MD. The primary goal of ADNI has been to test whether serial magnetic resonance imaging (MRI), PET, other biological markers, and clinical and neuropsychological assessment can be combined to measure the progression of mild cognitive impairment (MCI) and early AD.

Our study included 247 participants who had undergone concurrent (acquired within 6 months) baseline structural MRI, Aβ and FTP-PET scans, as well as concurrent follow-up MRI and FTP-PET scans (1.88 ±0.92 years). Participants had undergone baseline clinical evaluation and were classified as cognitively unimpaired (CU, $N = 134$) or cognitively impaired individuals (CI, $N = 113$; combining patients with mild cognitive impairment (MCI) and AD dementia). Additionally, longitudinal cognitive performance data measured using the Alzheimer's Disease Assessment Scale-Cognitive Subscale (ADAS-Cog 11) were available for CI individuals ($N = 110$; 2.31±1.09 years between assessments).

2.2. Image acquisition

MRI and PET scan acquisitions followed the same protocols as described in previous studies (Costoya-Sánchez et al., 2023). In brief, FTP-PET scans in ADNI were acquired using dynamic 3D acquisitions of six 5-min frames starting 75 min after injection of 370±10 % MBq. ADNI Aβ PET scans were acquired using dynamic 3D acquisitions of four 5-min frames starting 50 min after injection of 370±10 % MBq of [^{18}F]FTP or 90 min after the injection of 300±10 % MBq of [^{18}F]florbetaben. For this study, we used images in pre-processing level four as described by ADNI (https://adni.loni.usc.edu/methods/pet-analysis-method/pet-analysis/), which corresponds to co-registered and averaged PET scans, further reoriented to a standard image matrix and smoothed to 8 mm isotropic resolution.

T1 structural scans from ADNI were acquired on 3T scanners using an accelerated sagittal MPRAGE sequence with a spatial resolution of 1 mm^3. Each series in each exam underwent quality control following the steps described in detail in ADNI's MRI protocol (http://adni.loni.usc.edu/methods/mri-tool/mri-analysis/).

2.3. Neuroimaging processing

MRI scans were segmented using both FreeSurfer 7.1.1 and Statistical Parametric Mapping 12 (SPM12, Wellcome Department of Imaging

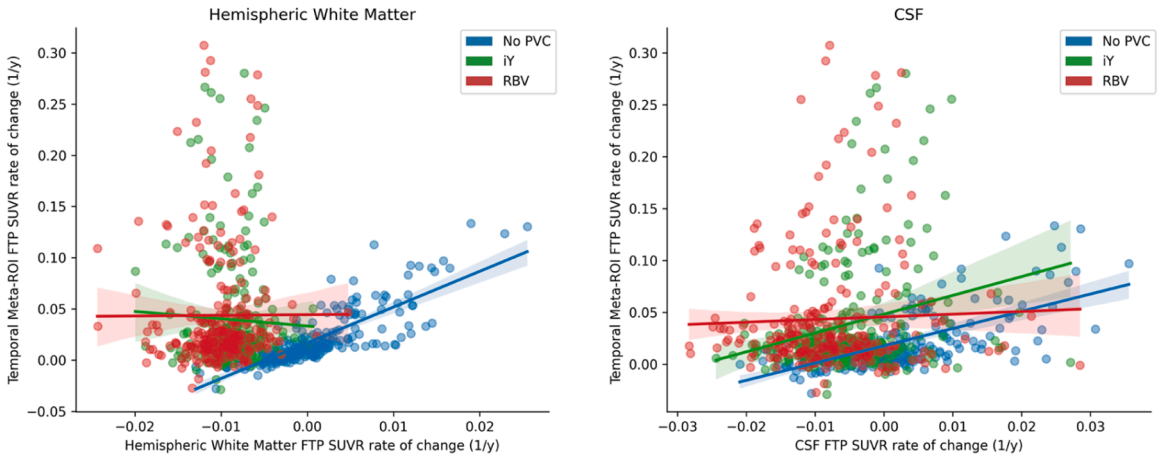

Fig. 1. FTP SUVRs rates of change relation in the temporal meta-ROI vs off-target ROIs (HemisW and CSF), including trend lines derived from linear regression.

Neuroscience, Institute of Neurology, London, UK) default pipelines. FreeSurfer's segmentation ROIs were merged to generate the masks for Braak I/II, III/IV, and V/VI ROIs, as well as a previously defined temporal meta-ROI aimed at detecting early tau accumulation (Jack et al., 2017). Cortical volume measurements for these same ROIs were obtained from FreeSurfer's anatomical analysis. Additionally, FreeSurfer's output ROIs for the caudate, putamen, pallidum, thalamus, choroid plexus (ChPlex), hemispheric white matter (hemisW), cerebellar white matter (cerebW) and cerebrospinal fluid (CSF) were included as off-target ROIs (Baker et al., 2019; López-González et al., 2022).

FTP and Aβ PET scans were co-registered to the corresponding MRI scan using SPM12. Aβ PET load was quantified using the Centiloid scale following the guidelines proposed by (Klunk et al., 2015), and Aβ PET positivity was defined using a conservative threshold of 12 Centiloids.

FTP-PET scans were corrected for PVE using some of the most used PVC techniques for brain PET. First, we included the Meltzer's correction (Meltzer et al., 1990), which represents a simple deconvolution technique. Meltzer's PVC was implemented as previously described by (Jack et al., 2018). To this end, a binarized GM mask (tissue probability of 0.5 or higher) was derived from the SPM segmentation and smoothed using a gaussian filter matching FTP-PET image resolution (FWHM=8 mm). The FTP image was further deconvoluted using this image to obtain the PVE-corrected image. While this PVC has been previously proposed for longitudinal FTP-PET studies (Jack et al., 2018), it relies in assuming that signal outside the cortex equals to zero. Thus, this method corrects for the spill-out effect in boundary regions of the segmented GM (such as those right next to CSF), but it cannot remove the contributions from CSF and hemisW. Additionally, we tested two voxel-based techniques: the iterative Yang (iY) (Yang et al., 1996) and the region-based voxel-wise corrections (RBV) (Thomas et al., 2011). iY is a multi-region extension of the voxel-based correction developed by (Videen et al., 1988); and RBV is a modified version of the iY combined with the geometric transfer matrix method (Rousset et al., 1998). Both of these voxel-wise corrections were performed using the PETPVC toolbox (Thomas et al., 2016), combined with Baker's subject-specific atlas (Baker et al., 2017). The subject-specific atlas is derived by combining inputs from FreeSurfer's and SPM12 segmentations, and it includes cortical and off-target ROIs relevant for FTP-PET quantification. Following the recommendations from the authors, we used ROI configuration number 8 in the method publication for generating the subject atlases.

FTP SUVRs were then computed for all PVCs using the inferior cerebellar gray matter as the reference region, obtained from the SUIT cerebellar template (Diedrichsen, 2006).

2.4. Statistical analysis

To explore the effect of spill-in counts from off-target areas on longitudinal FTP SUVRs in cortical target ROIs (and their effect in the opposite direction), we computed correlations between SUVR rates of change in target areas (Braak areas and temporal meta-ROI) vs SUVR rates in off-target ROIs, and assessed the effect of using PVC methods on these correlations compared to the use of no PVC (Meltzer correction was not included in this analysis as it can only be applied to grey matter and is thus not available for off-target regions).

In addition, the performance of the PVC techniques was evaluated through their effect on group differences in FTP SUVR rates of change between CU and CI individuals, as well as between A- and A+ individuals. For this, linear models were applied for comparing groups (controlling for age and sex), using FTP SUVRs without PVC and after applying the different PVC techniques. The performance was evaluated using the corresponding effect sizes of group differences estimated as Cohen's d.

Finally, correlations between baseline FTP SUVR and rates of cortical volume change were computed using linear mixed models with subject-specific intercepts and slopes. Again, this analysis was carried out using FTP SUVRs without PVC and after applying the different PVC techniques. Similarly, correlations between baseline FTP SUVR and ADAS-Cog11 rate of changes were also estimated. Confidence intervals for all statistical estimates, such as R^2 estimates, were calculated using bootstrap ($N = 1000$), and compared using two-sample t-tests.

3. Results

3.1. Correlations between FTP SUVR rates in off-target and target ROIs

Fig. 1 and Table 1 show the correlations between FTP SUVR rates of change in the target areas (Braak and temporal meta-ROI) vs the off-target ROIs. Without applying PVC (Fig. 1, blue bars), we observed a significant correlation between SUVR rates in target and off-target regions, which was particularly strong for the hemisW (up to R^2=0.8) and CSF (up to R^2=0.4). When applying the iY or RBV corrections (Fig. 1, green and red bars), we observed significant decreases in the strength of the correlation ($p < 0.05$) for both methods for almost all combinations of off-target and target areas that showed strong correlations without PVC. Notably, this also includes significant R^2 reductions for the correlation between the ChPlex and Braak I/II ROIs. Supplementary Figure S1 provides example images of the results of each tested PVC.

Table 1
R-squared estimates with 95 % confidence intervals of the regression model between FTP SUVR rates of change of target and off-target ROIs. Statistically significantly ($p < 0.05$) lower R-squared estimates compared to those of 'No PVC' are highlighted in bold.

		Braak I/II	*Braak III/IV*	*Braak V/VI*	*Temporal Meta-ROI*
HemisW	*No PVC*	0.28 ± 0.13	0.67 ± 0.09	0.82 ± 0.04	0.66 ± 0.09
	iY	**0.09 ± 0.07**	**0.00 ± 0.02**	**0.08 ± 0.06**	**0.00 ± 0.01**
	RBV	**0.07 ± 0.06**	**0.00 ± 0.01**	**0.04 ± 0.05**	**0.00 ± 0.01**
Pallidum	*No PVC*	0.10 ± 0.10	0.06 ± 0.06	0.10 ± 0.08	0.06 ± 0.06
	iY	**0.01 ± 0.03**	**0.00 ± 0.01**	**0.00 ± 0.02**	**0.00 ± 0.01**
	RBV	**0.01 ± 0.03**	**0.00 ± 0.01**	**0.00 ± 0.02**	**0.00 ± 0.01**
Thalamus	*No PVC*	0.04 ± 0.08	0.01 ± 0.03	0.05 ± 0.05	0.01 ± 0.03
	iY	0.02 ± 0.03	0.00 ± 0.01	0.03 ± 0.04	0.00 ± 0.01
	RBV	0.01 ± 0.03	0.00 ± 0.01	0.02 ± 0.03	0.00 ± 0.01
CSF	*No PVC*	0.28 ± 0.10	0.41 ± 0.11	0.43 ± 0.11	0.42 ± 0.11
	iY	**0.04 ± 0.05**	**0.06 ± 0.05**	**0.02 ± 0.04**	**0.06 ± 0.05**
	RBV	**0.01 ± 0.02**	**0.00 ± 0.01**	**0.00 ± 0.01**	**0.00 ± 0.01**
ChPlex	*No PVC*	0.06 ± 0.05	0.01 ± 0.02	0.02 ± 0.03	0.01 ± 0.02
	iY	**0.01 ± 0.02**	0.01 ± 0.03	0.01 ± 0.02	0.01 ± 0.02
	RBV	**0.01 ± 0.02**	0.01 ± 0.02	0.01 ± 0.02	0.01 ± 0.02
Caudate	*No PVC*	0.02 ± 0.04	0.00 ± 0.01	0.01 ± 0.02	0.00 ± 0.01
	iY	0.00 ± 0.03	0.00 ± 0.01	0.00 ± 0.01	0.00 ± 0.01
	RBV	0.01 ± 0.03	0.00 ± 0.02	0.00 ± 0.01	0.00 ± 0.02
CerebW	*No PVC*	0.01 ± 0.02	0.00 ± 0.02	0.02 ± 0.03	0.00 ± 0.02
	iY	0.00 ± 0.01	0.00 ± 0.01	0.01 ± 0.03	0.00 ± 0.02
	RBV	0.00 ± 0.01	0.00 ± 0.01	0.00 ± 0.02	0.00 ± 0.01
Putamen	*No PVC*	0.07 ± 0.08	0.13 ± 0.08	0.19 ± 0.10	0.13 ± 0.08
	iY	**0.02 ± 0.05**	**0.06 ± 0.05**	**0.04 ± 0.06**	**0.06 ± 0.06**
	RBV	0.03 ± 0.06	**0.07 ± 0.06**	**0.04 ± 0.07**	**0.07 ± 0.06**

3.2. Group differences in FTP SUVR rates of change

Fig. 2 shows differences in FTP SUVR rates of change between CU and CI individuals. Supplementary Table S1 provides additional information on the CU/CI group demographics. For the RBV correction, we observed significant increases in effect size compared to no PVC data for all target ROIs (Braak I/II $\Delta d=0.17\pm0.15$, $p = 0.01$; Braak III/IV $\Delta d=0.08\pm0.06$, $p = 0.01$; Braak V/VI $\Delta d=0.17\pm0.14$, $p = 0.006$; Temporal Meta-ROI $\Delta d=0.09\pm0.06$ $p = 0.004$). The iY correction also showed significant increases in effect sizes for all ROIs except for Braak I/II (Braak I/II $\Delta d=0.06\pm0.13$, $p = 0.18$; Braak III/IV $\Delta d=0.05\pm0.05$, $p = 0.03$; Braak V/VI $\Delta d=0.15\pm0.13$, $p = 0.008$; temporal meta-ROI $\Delta d=0.06\pm0.06$ $p = 0.04$), and the Meltzer's correction showed significant increases in effect size for all ROIs except for Braak III/IV (Braak I/II $\Delta d=0.31\pm0.13$, $p < 0.001$; Braak III/IV $\Delta d=0.07\pm0.08$, $p = 0.05$; Braak V/VI $\Delta d=0.16\pm0.12$, $p = 0.15$; Temporal Meta-ROI $\Delta d=0.08\pm0.08$ $p = 0.04$).

Fig. 3 displays the differences in FTP SUVR rate of change between the A- and A+ groups. Supplementary Table S1 provides additional information on the A-/A+ group demographics. Group differences without PVC were larger across all ROIs compared to those found for CU/CI. In contrast with what we observed in the CU/CI analysis, none of the PVC methods resulted in significant effect size increases between A-/A+ individuals compared to no PVC data. Only the Meltzer correction showed increased group differences for some areas, although none of them were statistically significant (Braak I/II $\Delta d=0.10\pm0.25$, $p = 0.07$; Braak III/IV $\Delta d=-0.01\pm0.12$, $p = 0.40$; Braak V/VI $\Delta d=0.01\pm0.12$, $p = 0.43$; Temporal Meta-ROI $\Delta d=0.00\pm0.12$ $p = 0.42$).

3.3. Baseline FTP SUVR and rates of cortical volume change

Fig. 4 shows the R-squared estimate between baseline FTP SUVR and longitudinal cortical volume rate of change in the same target ROI. RBV and iY showed significantly higher R-squared for Braak III/IV (iY: $\Delta R^2=0.02\pm0.01$, $p = 0.006$; RBV: $\Delta R^2=0.02\pm0.02$, $p = 0.004$) and the Temporal Meta-ROI (iY: $\Delta R^2=0.0.2 \pm 0.02$, $p = 0.002$; RBV: $\Delta R^2=0.02 \pm 0.02$ $p = 0.001$), but not for the other ROIs. Meltzer did not result in a significant R^2 increase for any region.

3.4. Baseline FTP SUVR and ADAS-Cog 11 rate of change

Fig. 5 shows the R-squared estimate between baseline FTP SUVR and the rate of change of the ADAS-Cog 11 score in CI individuals. All PVC techniques resulted in significantly higher R-squared for Braak III/IV (Meltzer: $\Delta R^2=0.04\pm0.03$, $p = 0.01$; iY: $\Delta R^2=0.03\pm0.03$, $p = 0.02$; RBV: $\Delta R^2=0.04\pm0.04$, $p = 0.01$) and for the Temporal Meta-ROI (Meltzer: $\Delta R^2=0.04\pm0.03$ $p = 0.01$; iY: $\Delta R^2=0.03\pm0.03$, $p = 0.02$; RBV: $\Delta R^2=0.04\pm0.04$ $p = 0.01$). Similar to the cortical volume analysis, no significant differences were observed for the Braak I/II nor Braak V/VI ROIs.

4. Discussion

The main aim of our study was to assess whether different PVC approaches provide the expected benefits in longitudinal FTP-PET studies. To this end, we first analysed the impact of off-target uptake on measured tau accumulation rates of change in cortical target areas. Here, we observed that variation in hemisW signal was a significant contributor to the measured rates of change in all the target ROIs (Braak and Temporal Meta-ROI) ($R^2=0.28$ for Braak I/II, $R^2>0.66$ for other target areas). This result aligns with previously reported data on cross-sectional studies that locate the hemisW as the main contributor to the partial volume effect on cortical areas (Baker et al., 2019). We observed that this correlation almost completely disappeared after applying voxel-wise PVC methods, especially for Braak III/IV and the Temporal Meta-ROI ($R^2=0.00$). CSF signal also had a moderate effect on the quantification of FTP SUVR rates of change in target areas ($R^2>0.28$), which is also in good agreement with observations from previous cross-sectional studies (López-González et al., 2022). Similar to hemisW, this effect was largely attenuated when applying PVC ($R^2<0.06$). This pattern of findings was similar for all off-target ROIs, but the contribution of off-target regions other than hemisW and CSF to longitudinal outcome measurements was very low. Correlations between Braak areas and distant areas such as the putamen and pallidum were also observed, probably related with PVE from hemisW to these adjacent regions (López-González et al., 2022). Interestingly, these correlations were attenuated but persisted after PVC. This is a recurrent finding in previous cross-sectional studies (Baker et al., 2019; López-González et al., 2022), where the authors hypothesized that these correlations might be related to the existence of biological or tracer-related contributions that cannot be fully removed with PVC.

Aside from the benefits observed on reducing the correlations between target and off-target regions, PVC comes with side effects such as

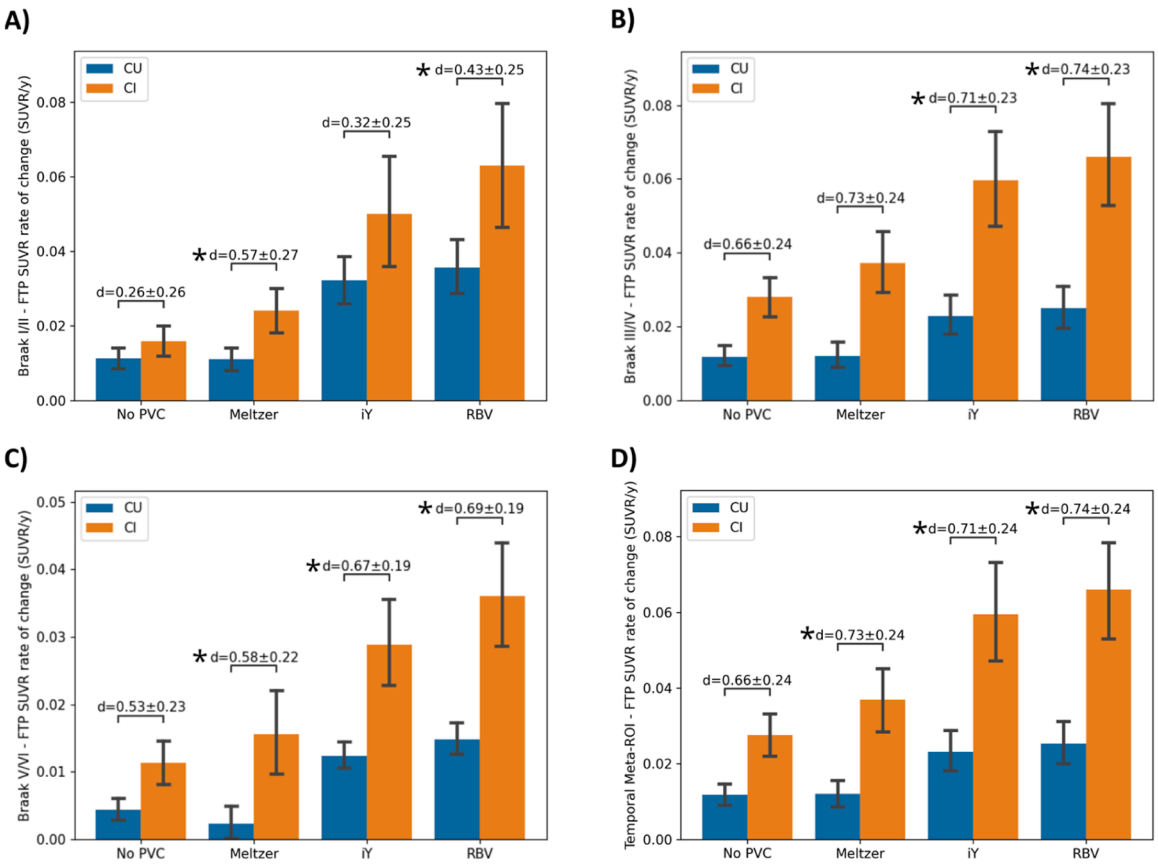

Fig. 2. Group differences measured as Cohen's d in regional FTP SUVR rate of change (mean ± 95 % confidence intervals) between CU and CI individuals. Error bars indicate the 95 % confidence interval for FTP SUVR rates of change. Asterisk indicates effect sizes (d) significantly larger than the 'No PVC' effect size at $p < 0.05$. A) Braak I/II. B) Braak III/IV. C) Braak V/VI. D) Temporal Meta-ROI.

increased noise, that may partially dampen the beneficial effects of PVC techniques when measurement variability plays a role. This may be especially critical for AD studies, where experiments usually try to measure how tau accumulation rates differ between different groups of interest, sometimes using short time-spans (Costoya-Sánchez et al., 2023; Yoon et al., 2022). To assess the possible benefits of PVC in these cases, we conducted complementary analyses assessing the effect of the PVC techniques on group-level analyses of FTP SUVR rates of change in the target regions between CU/CI and A-/A+ individuals, two common pairs of groups of study. For the CU/CI analysis, we observed a consistently good performance of the RBV method, resulting in increased group differences in measured FTP SUVR rates of change across all cortical target regions and displaying the largest increases in effect size. Meltzer's correction appeared to be the second best, slightly outperforming the iY's. The better performance of RBV compared to iY was particularly interesting, as both showed a similar ability to remove the correlation between off-target and target uptake. We hypothesize that RBV may provide a better noise handling, and thus a better group separation overall. Regarding the differences between iY and Meltzer's, these may be due to a better performance of the Meltzer's method in correcting the effects of atrophy between groups (Tabatabaei-Jafari et al., 2015). Overall, we can state that PVC generally showed a modest but still significant improvement (i.e. higher effect size) for assessing the differences in longitudinal FTP SUVR rates of change between the CU/CI groups. By contrast, our findings do not support a similar beneficial effect of PVC for improving detection of group differences in FTP SUVR rates of change between A- and A+ individuals. It is interesting to note that in this case, even the data without PVC already showed considerably larger group differences compared to the CU vs CI comparison, and these large group differences were not further increased by PVC. The fact that the differences in longitudinal tau accumulation between the A- and A+ individuals are larger than between CU and CI individuals can be expected, since cognitive impairment in AD occurs mainly after A + T+ is reached, while CU subjects may be A+ and accumulating tau prior to measurable effects on cognition. Thus, our results suggest that PVC may be more beneficial in scenarios where differences between groups are expected to be subtle. This might be due to the relatively large improvement in discrimination power that reducing spill-in effects to target regions has on groups with similar distributions.

We also evaluated the effect of PVC on the correlations between baseline FTP SUVR measurements and prospective cortical volume and cognitive performance decline. Here, we found significant increases in correlation strength after PVC for some of the cortical target ROIs, specifically Braak III/IV and the Temporal Meta-ROIs. In both cases, RBV showed a slightly higher performance than the iY correction, although the differences were minor (<0.01 in R^2). Meltzer's correction only showed a significant improvement for these ROIs in the cognitive decline analysis, with a performance increase in between that of the iY and RBV corrections.

To the best of our knowledge, ours is the first study systematically evaluating the role of off-target binding on longitudinal FTP-PET measurements. In this regard, our study revealed a significant correlation between off-target and measured rates of change in tau accumulation. As for previous cross-sectional studies, the main contributors were the hemispheric white matter and, to a lesser extent, the CSF signal. Among the tested PVCs, voxel-wise corrections (especially the RBV) successfully removed most of this PVE effect, providing significant improvements on reducing the correlation between off-target uptake and measured rates of change estimations in tau accumulation. In a recent study (Schwarz et al., 2021), the authors compared a total of 415 different quantification

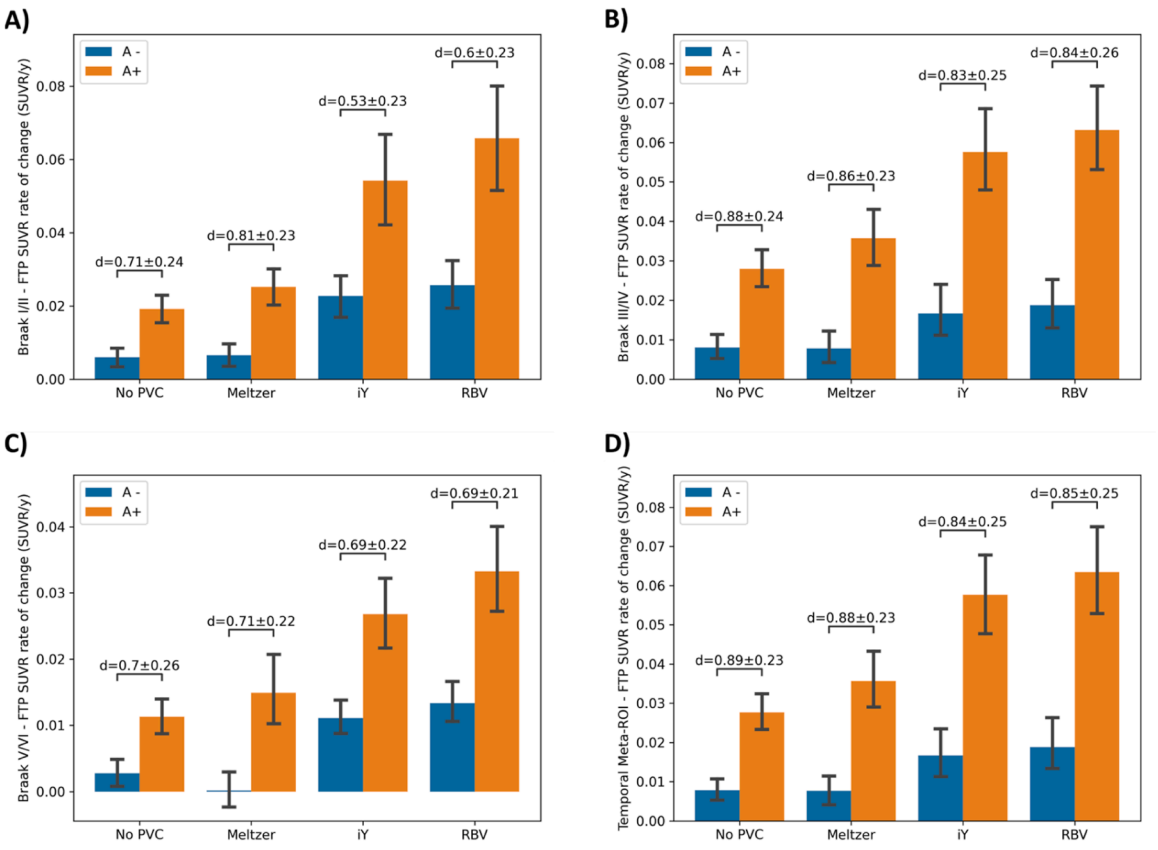

Fig. 3. Group differences in regional FTP SUVR rate of change (mean ± 95 % confidence intervals) between A- and A+ individuals. Differences are expressed as effect size (Cohen's d). Error bars indicate the 95 % confidence interval for FTP SUVR rates of change. No effect sizes were significantly larger than the 'No PVC' effect size. A) Braak I/II. B) Braak III/IV. C) Braak V/VI. D) Temporal Meta-ROI.

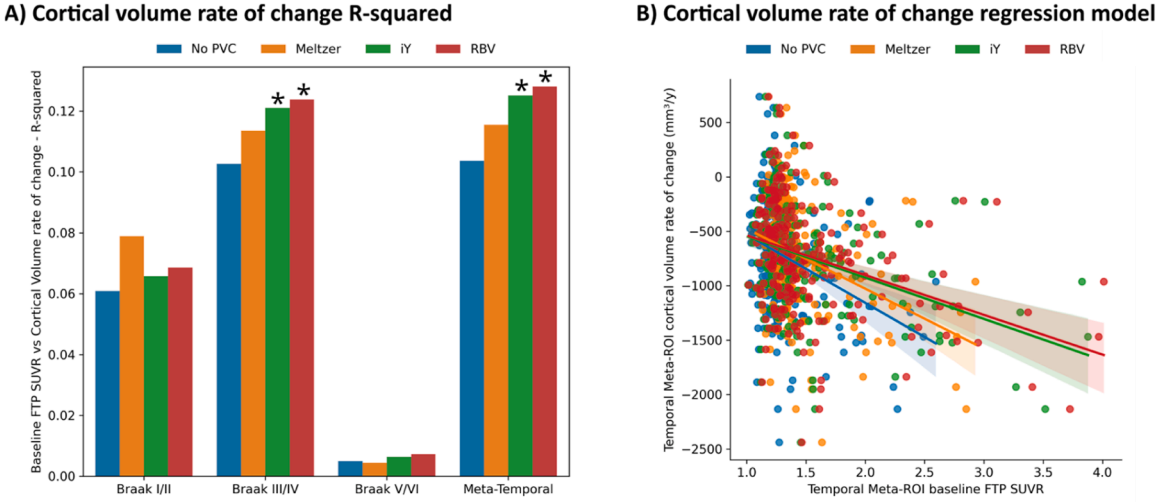

Fig. 4. R-squared of the linear regression model between baseline FTP SUVR and cortical volume rate of change for the same ROI. Asterisk indicates a significantly larger R^2 compared to that of 'No PVC' for $p < 0.05$.

pipelines, including variations on PVC methodology. While the multi-parametric approach of the study makes it difficult to reach solid conclusions about the impact of PVC, the best performing pipelines consistently included 2-class voxel-based PVC. Here we observed that complex voxel-based approaches provided the best results, but a simple deconvolution PVC may provide similar results in some scenarios. However, in contrast with common assumptions, we observed a very limited benefit of applying PVC for tasks involving the measurement of group-level longitudinal differences, where the increase in noise and variability caused by the correction might deteriorate the effectivity of the analysis. These findings are particularly relevant for the estimations of sample sizes and analysis methodologies of longitudinal group studies and their statistical power.

Regarding the limitations of this work, the most relevant is the lack of a ground-truth for the estimation of true rates of tau accumulation. Ours and other studies have associated higher effect sizes with a better

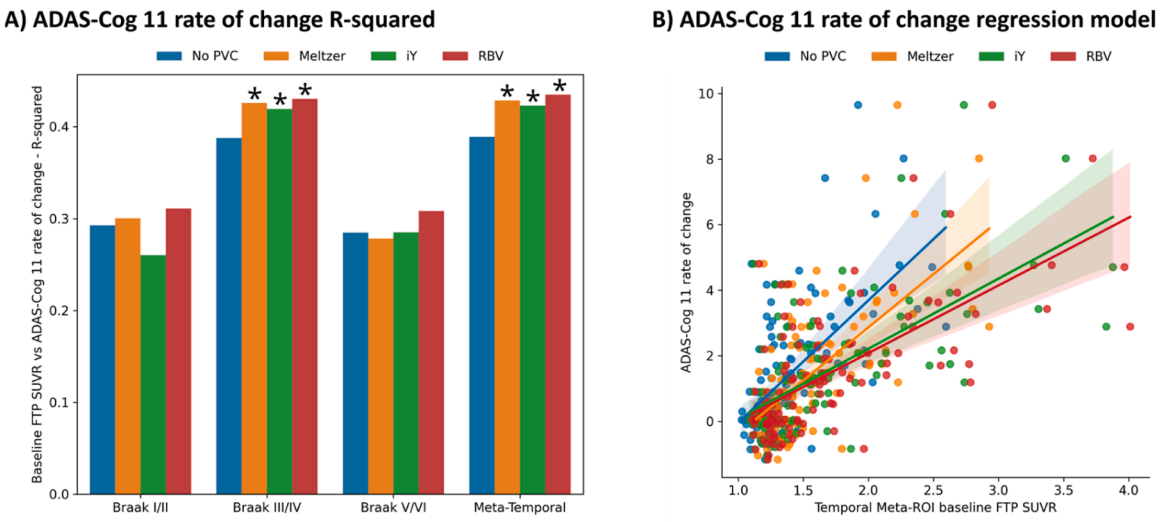

Fig. 5. R-squared of the linear regression model between baseline FTP SUVR and the ADAS-Cog 11 score rate of change for CI individuals. 3 participants were excluded due to the lack of follow-up ADAS-Cog 11 data. Asterisk indicates a significantly larger R-squared compared to that of 'No PVC' for $p < 0.05$.

measurement; however, this is based on an a priori assumption, and to what extent this increased effect size reflect an improvement in accuracy remains unknown. Previous cross-sectional studies analysing the effect of PVC in the correlation between ante-mortem image-based pathological loads with postmortem measures obtained at autopsy have shown no significant benefit from PVC (Minhas et al., 2018), but autopsy measurements reflect total, end-point accumulation, which may be poorly linked with the longitudinal rates of accumulation. To date, gold-standard for tau rates of accumulation is not available. On the other hand, previous cross-sectional studies (Minhas et al., 2018; Weigand et al., 2022) have suggested that the correlation between atrophy and PET signal might be artificially increased by the overestimation of radiotracer uptake caused by some PVC techniques. This perceived increase in the statistical power of longitudinal quantification should therefore be further investigated to better assess the exact benefits of the use of PVC. Additionally, we have only included a limited set of PVC techniques. Future studies might benefit from the inclusion of a wider range of PVC techniques. Particularly, we expect that analytical techniques that allow the inclusion of more off-target regions (hemisW, CSF) may perform similarly to what we observed with voxel-based corrections (Gonzalez-Escamilla et al., 2017). Recently, deep learning methods applied to image analysis are giving birth to a new generation of PVC techniques (Matsubara et al., 2022). To what extent the exposed limitations of PVC can be solved by these new approaches is a prospect for future studies. Moreover, we have limited our study to the ADNI cohort and only included PET scans pre-processed following ADNI's level 4 pipeline. A better characterization of different PVC techniques in longitudinal studies might benefit from the inclusion of a variety of cohorts, and since the specifics of the preprocessing pipeline might also affect FTP-PET quantification (Schwarz et al., 2021), comparisons of PVCs across more diverse sets of processing pipelines and cohorts may improve our understanding of the impact of PVC . Finally, the findings reported in this study are specific to FTP and cannot be easily extrapolated to other tau PET radiotracers with different off-target uptake characteristics, for which similar studies should be carried out.

5. Conclusions

Quantification of longitudinal changes in cortical FTP-PET is heavily influenced by PVE from off-target regions, primarily from signal in the hemispheric white matter and the CSF. PVC methods proved to be effective in reducing this confounding effect. However, the use of PVC techniques showed very limited benefits in increasing statistical power when studying group-level differences in longitudinal FTP SUVR measurements.

Consent for publication

Not applicable

Funding

The project that gave rise to these results received the support of a fellowship from "la Caixa" Foundation (ID 100010434). The fellowship code is LCF/BQ/DR20/11790012. This work is partly funded by the public projects funded by ERDF: PI19/01315 (ISCIII) and EAPA_791/2018 NeuroATLANTIC (UE Interreg). Jesús Silva-Rodríguez is a Sara Borrell fellow (CD21/00067). MJG is supported by the "Miguel Servet" program (CP19/00031) and a research grant (PI20/00613) of the Instituto de Salud Carlos III-Fondo Europeo de Desarrollo Regional (ISCIII-FEDER). MS is supported by the Knut and Alice Wallenberg Foundation (Wallenberg Centre for Molecular and Translational Medicine; KAW2014.0363), the Swedish Research Council (2017–02869 2021–02678 and 2021–06545), the Swedish state under the agreement between the Swedish government and the County Councils, the ALF-agreement (ALFGBG-813971 and ALFGBG-965326), the Swedish Brain Foundation (FO2021–0311) and the Swedish Alzheimer Foundation (AF-740191).

Data availability

Patient data used in the preparation of this article were obtained from the Alzheimer's Disease Neuroimaging Initiative (ADNI) database. Data from the ADNI is open and can be obtained from the ADNI data repositories. Code use in this article will be made available upon request.

Ethics statement

The ADNI studies were conducted according to Good Clinical Practice guidelines, US 21CFR Part 50– Protection of Human Subjects, and Part 56 – Institutional Review Boards (IRBs) / Research Ethics Boards (REBs), and pursuant to state and federal HIPAA regulations. Written informed consent for the study was obtained from all participants and/or authorized representatives.

CRediT authorship contribution statement

Alejandro Costoya-Sánchez: Writing – original draft, Formal analysis, Data curation. **Alexis Moscoso:** Writing – review & editing, Conceptualization. **Tomás Sobrino:** Writing – review & editing. **Álvaro Ruibal:** Writing – review & editing. **Michel J. Grothe:** Writing – review & editing. **Michael Schöll:** Writing – review & editing. **Jesús Silva-Rodríguez:** Writing – review & editing, Supervision, Conceptualization. **Pablo Aguiar:** Writing – review & editing, Conceptualization.

Declaration of competing interest

None.

Acknowledgements

Data collection and sharing for this project was funded by the Alzheimer's Disease Neuroimaging Initiative (ADNI) (National Institutes of Health Grant U01 AG024904) and DOD ADNI (Department of Defense award number W81XWH-12-2-0012). ADNI is funded by the National Institute on Aging, the National Institute of Biomedical Imaging and Bioengineering, and through generous contributions from the following: AbbVie, Alzheimer's Association; Alzheimer's Drug Discovery Foundation; Araclon Biotech; BioClinica, Inc.; Biogen; Bristol-Myers Squibb Company; CereSpir, Inc.; Cogstate; Eisai Inc.; Elan Pharmaceuticals, Inc.; Eli Lilly and Company; EuroImmun; F. Hoffmann-La Roche Ltd and its affiliated company Genentech, Inc.; Fujirebio; GE Healthcare; IXICO Ltd.; Janssen Alzheimer Immunotherapy Research & Development, LLC.; Johnson & Johnson Pharmaceutical Research & Development LLC.; Lumosity; Lundbeck; Merck & Co., Inc.; Meso Scale Diagnostics, LLC.; NeuroRx Research; Neurotrack Technologies; Novartis Pharmaceuticals Corporation; Pfizer Inc.; Piramal Imaging; Servier; Takeda Pharmaceutical Company; and Transition Therapeutics. The Canadian Institutes of Health Research is providing funds to support ADNI clinical sites in Canada. Private sector contributions are facilitated by the Foundation for the National Institutes of Health (www.fnih.org). The grantee organization is the Northern California Institute for Research and Education, and the study is coordinated by the Alzheimer's Therapeutic Research Institute at the University of Southern California. ADNI data are disseminated by the Laboratory for Neuro Imaging at the University of Southern California.

Supplementary materials

Supplementary material associated with this article can be found, in the online version, at doi:10.1016/j.neuroimage.2024.120537.

References

Aston, J.A.D., Cunningham, V.J., Asselin, M.C., Hammers, A., Evans, A.C., Gunn, R.N., 2002. Positron emission tomography partial volume correction: estimation and algorithms. J. Cereb. Blood Flow Metab. 22, 1019–1034. https://doi.org/10.1097/00004647-200208000-00014.

Baker, S.L., Harrison, T.M., Maass, A., La Joie, R., Jagust, W.J., 2019. Effect of off-target binding on ^{18}F-Flortaucipir variability in healthy controls across the life span. J. Nucl. Med. 60, 1444–1451. https://doi.org/10.2967/jnumed.118.224113.

Baker, S.L., Maass, A., Jagust, W.J., 2017. Considerations and code for partial volume correcting [18 F]-AV-1451 tau PET data. Data Brief 15, 648–657. https://doi.org/10.1016/j.dib.2017.10.024.

Bischof, G.N., Dodich, A., Boccardi, M., Van Eimeren, T., Festari, C., Barthel, H., Hansson, O., Nordberg, A., Ossenkoppele, R., Sabri, O., Giovanni, B.F.G., Garibotto, V., Drzezga, A., 2021. Clinical validity of second-generation tau PET tracers as biomarkers for Alzheimer's disease in the context of a structured 5-phase development framework. Eur. J. Nucl. Med. Mol. Imaging 48, 2110–2120. https://doi.org/10.1007/s00259-020-05156-4.

Chien, D.T., Bahri, S., Szardenings, A.K., Walsh, J.C., Mu, F., Su, M.Y., Shankle, W.R., Elizarov, A., Kolb, H.C., 2013. Early clinical PET Imaging results with the novel PHF-Tau radioligand [F-18]-T807. J. Alzheimers Dis. 34, 457–468. https://doi.org/10.3233/JAD-122059.

Costoya-Sánchez, A., Moscoso, A., Silva-Rodríguez, J., Pontecorvo, M.J., Devous, M.D., Aguiar, P., Schöll, M., Grothe, M.J., 2023. Increased medial temporal tau positron emission tomography uptake in the absence of amyloid-β positivity. JAMA Neurol. https://doi.org/10.1001/jamaneurol.2023.2560.

Diedrichsen, J., 2006. A spatially unbiased atlas template of the human cerebellum. Neuroimage 33, 127–138. https://doi.org/10.1016/j.neuroimage.2006.05.056.

Erlandsson, K., Buvat, I., Pretorius, P.H., Thomas, B.A., Hutton, B.F., 2012. A review of partial volume correction techniques for emission tomography and their applications in neurology, cardiology and oncology. Phys. Med. Biol. 57, R119–R159. https://doi.org/10.1088/0031-9155/57/21/R119.

Gogola, A., Minhas, D.S., Villemagne, V.L., Cohen, A.D., Mountz, J.M., Pascoal, T.A., Laymon, C.M., Mason, N.S., Ikonomovic, M.D., Mathis, C.A., Snitz, B.E., Lopez, O.L., Klunk, W.E., Lopresti, B.J., 2022. Direct comparison of the tau PET Tracers ^{18}F-Flortaucipir and ^{18}F-MK-6240 in human subjects. J. Nucl. Med. 63, 108–116. https://doi.org/10.2967/jnumed.120.254961.

Gonzalez-Escamilla, G., Lange, C., Teipel, S., Buchert, R., Grothe, M.J., 2017. PETPVE12: an SPM toolbox for partial volume effects correction in brain PET Application to amyloid imaging with AV45-PET. Neuroimage 147, 669–677. https://doi.org/10.1016/j.neuroimage.2016.12.077.

Jack, C.R., Wiste, H.J., Schwarz, C.G., Lowe, V.J., Senjem, M.L., Vemuri, P., Weigand, S.D., Therneau, T.M., Knopman, D.S., Gunter, J.L., Jones, D.T., Graff-Radford, J., Kantarci, K., Roberts, R.O., Mielke, M.M., Machulda, M.M., Petersen, R.C., 2018. Longitudinal tau PET in ageing and Alzheimer's disease. Brain 141, 1517–1528. https://doi.org/10.1093/brain/awy059.

Jack, C.R., Wiste, H.J., Weigand, S.D., Therneau, T.M., Lowe, V.J., Knopman, D.S., Gunter, J.L., Senjem, M.L., Jones, D.T., Kantarci, K., Machulda, M.M., Mielke, M.M., Roberts, R.O., Vemuri, P., Reyes, D.A., Petersen, R.C., 2017. Defining imaging biomarker cut points for brain aging and Alzheimer's disease. Alzheimers Dement 13, 205–216. https://doi.org/10.1016/j.jalz.2016.08.005.

Klunk, W.E., Koeppe, R.A., Price, J.C., Benzinger, T.L., Devous, M.D., Jagust, W.J., Johnson, K.A., Mathis, C.A., Minhas, D., Pontecorvo, M.J., Rowe, C.C., Skovronsky, D.M., Mintun, M.A., 2015. The Centiloid Project: standardizing quantitative amyloid plaque estimation by PET. Alzheimers Dement 11, 1. https://doi.org/10.1016/j.jalz.2014.07.003.

Lemoine, L., Gillberg, P.G., Svedberg, M., Stepanov, V., Jia, Z., Huang, J., Nag, S., Tian, H., Ghetti, B., Okamura, N., Higuchi, M., Halldin, C., Nordberg, A., 2017. Comparative binding properties of the tau PET tracers THK5117, THK5351, PBB3, and T807 in postmortem Alzheimer brains. Alzheimers Res. Ther. 9, 96. https://doi.org/10.1186/s13195-017-0325-z.

Leuzy, A., Chiotis, K., Lemoine, L., Gillberg, P.G., Almkvist, O., Rodriguez-Vieitez, E., Nordberg, A., 2019. Tau PET imaging in neurodegenerative tauopathies Still a challenge. Mol. Psychiatry 24, 1112–1134. https://doi.org/10.1038/s41380-018-0342-8.

López-González, F.J., Costoya-Sánchez, A., Paredes-Pacheco, J., Moscoso, A., Silva-Rodríguez, J., Aguiar, P., 2022. Impact of spill-in counts from off-target regions on [18F]Flortaucipir PET quantification. Neuroimage 259, 119396. https://doi.org/10.1016/j.neuroimage.2022.119396.

Lu, Y., Toyonaga, T., Naganawa, M., Gallezot, J.D., Chen, M.K., Mecca, A.P., Van Dyck, C.H., Carson, R.E., 2021. Partial volume correction analysis for 11C-UCB-J PET studies of Alzheimer's disease. Neuroimage 238, 118248. https://doi.org/10.1016/j.neuroimage.2021.118248.

Matsubara, K., Ibaraki, M., Kinoshita, T., for the Alzheimer's Disease Neuroimaging Initiative, 2022. DeepPVC: prediction of a partial volume-corrected map for brain positron emission tomography studies via a deep convolutional neural network. EJNMMI Phys. 9, 50. https://doi.org/10.1186/s40658-022-00478-8.

Meltzer, C.C., Leal, J.P., Mayberg, H.S., Wagner, H.N., Frost, J.J., 1990. Correction of PET data for partial volume effects in human cerebral cortex by MR imaging. J. Comput. Assist. Tomogr. 14, 561–570. https://doi.org/10.1097/00004728-199007000-00011.

Minhas, D.S., Price, J.C., Laymon, C.M., Becker, C.R., Klunk, W.E., Tudorascu, D.L., Abrahamson, E.E., Hamilton, R.L., Kofler, J.K., Mathis, C.A., Lopez, O.L., Ikonomovic, M.D., 2018. Impact of partial volume correction on the regional correspondence between in vivo [C-11]PiB PET and postmortem measures of Aβ load. NeuroImage Clin. 19, 182–189. https://doi.org/10.1016/j.nicl.2018.04.007.

Ossenkoppele, R., Smith, R., Mattsson-Carlgren, N., Groot, C., Leuzy, A., Strandberg, O., Palmqvist, S., Olsson, T., Jögi, J., Stormrud, E., Cho, H., Ryu, Y.H., Choi, J.Y., Boxer, A.L., Gorno-Tempini, M.L., Miller, B.L., Soleimani-Meigooni, D., Iaccarino, L., La Joie, R., Baker, S., Borroni, E., Klein, G., Pontecorvo, M.J., Devous, M.D., Jagust, W.J., Lyoo, C.H., Rabinovici, G.D., Hansson, O., 2021. Accuracy of tau positron emission tomography as a prognostic marker in preclinical and prodromal alzheimer disease: a head-to-head comparison against amyloid positron emission tomography and magnetic resonance imaging. JAMA Neurol. 78, 961. https://doi.org/10.1001/jamaneurol.2021.1858.

Rousset, O.G., Ma, Y., Evans, A.C., 1998. Correction for partial volume effects in PET: principle and validation. J. Nucl. Med. 39, 904–911.

Schöll, M., Lockhart, S.N., Schonhaut, D.R., O'Neil, J.P., Janabi, M., Ossenkoppele, R., Baker, S.L., Vogel, J.W., Faria, J., Schwimmer, H.D., Rabinovici, G.D., Jagust, W.J., 2016. PET imaging of tau deposition in the aging human brain. Neuron 89, 971–982. https://doi.org/10.1016/j.neuron.2016.01.028.

Schultz, S.A., Gordon, B.A., Mishra, S., Su, Y., Perrin, R.J., Cairns, N.J., Morris, J.C., Ances, B.M., Benzinger, T.L.S., 2018. Widespread distribution of tauopathy in preclinical Alzheimer's disease. Neurobiol. Aging 72, 177–185. https://doi.org/10.1016/j.neurobiolaging.2018.08.022.

Schwarz, C.G., Therneau, T.M., Weigand, S.D., Gunter, J.L., Lowe, V.J., Przybelski, S.A., Senjem, M.L., Botha, H., Vemuri, P., Kantarci, K., Boeve, B.F., Whitwell, J.L., Josephs, K.A., Petersen, R.C., Knopman, D.S., Jack, C.R., 2021. Selecting software pipelines for change in flortaucipir SUVR: balancing repeatability and group

separation. Neuroimage 238, 118259. https://doi.org/10.1016/j.neuroimage.2021.118259.

Soleimani-Meigooni, D.N., Iaccarino, L., La Joie, R., Baker, S., Bourakova, V., Boxer, A.L., Edwards, L., Eser, R., Gorno-Tempini, M.L., Jagust, W.J., Janabi, M., Kramer, J.H., Lesman-Segev, O.H., Mellinger, T., Miller, B.L., Pham, J., Rosen, H.J., Spina, S., Seeley, W.W., Strom, A., Grinberg, L.T., Rabinovici, G.D., 2020. 18F-flortaucipir PET to autopsy comparisons in Alzheimer's disease and other neurodegenerative diseases. Brain 143, 3477–3494. https://doi.org/10.1093/brain/awaa276.

Tabatabaei-Jafari, H., Shaw, M.E., Cherbuin, N., 2015. Cerebral atrophy in mild cognitive impairment: a systematic review with meta-analysis. Alzheimers Dement. Diagn. Assess Dis. Monit. 1, 487–504. https://doi.org/10.1016/j.dadm.2015.11.002.

Teng, E., Manser, P.T., Pickthorn, K., Brunstein, F., Blendstrup, M., Sanabria Bohorquez, S., Wildsmith, K.R., Toth, B., Dolton, M., Ramakrishnan, V., Bobbala, A., Sikkes, S.A.M., Ward, M., Fuji, R.N., Kerchner, G.A., Tauriel Investigators, Farnbach, P., Kyndt, C., O'Brien, T., Yassi, N., Schwartz, R., Lieten, S., Vandenberghe, R., Vanhee, F., Bergeron, R., Black, S., Cohen, S., Frank, A., Nisker, W., Tartaglia, M.C., Justesen, A., Alexandersen, P., Nielsen, S., Areovimata, A., Anthony, P., Belliard, S., Blanc, F., Ceccaldi, M., Dubois, B., Krolak-Salmon, P., Mollion, H., Pasquier, F., Grimmer, T., Kottke-Arbeiter, M.E., Laske, C., Peters, O., Polivka, D., Von Arnim, C., Bruno, G., De Lena, C., Cassetta, E., Centonze, D., Logroscino, G., Dautzenberg, P., Rutgers, S., Prins, N., Czarnecki, M., Dobryniewski, J., Ilkowski, J., Klodowska, G., Krygowska-Wajs, A., Kucharski, R., Mickielewicz, A., Ratajczak, M., Zboch, M., Zielinski, T., Abizanda Soler, P., Agüera Morales, E., Baquero Toledo, M., Blesa González, R., Boada Rovira, M., Del Olmo Rodriguez, A., Krupinski, J., Linazasoro Cristobal, G., López Arrieta, J., Riverol Fernandez, M., Sanchez Del Valle Diaz, R., Viñuela Fernandez, F., Jonsson, M., Östlund, H., MacSweeney, J.E., Mummery, C., Agronin, M., Ala, T., Bond, W., Schaerf, F., Brody, M., Edwards, K., Forchetti, C., Sood, A., Geldmacher, D., Goldstein, M., Goodman, I., Hart, D., Honig, L., Justiz, W., Levey, A., Losk, S., Marshall, G., Martinez, W., McAllister, P., McElveen, W.A., Maldonado-Robles, O., Murphy, C., Nair, M., Nair, A., Omidvar, O., Oskooilar, N., Porsteinsson, A., Rosenbloom, M., Russell, D., Sajjadi, S.A., Pierce, A., Salloway, S., Sha, S., Shah, R., Sharma, S., Smith, W., Stein, L., Stoukides, J., Thein, S., Turner, R., Watson, D., Weisman, D., 2022. Safety and efficacy of semorinemab in individuals with prodromal to mild alzheimer disease: a randomized clinical trial. JAMA Neurol. 79, 758. https://doi.org/10.1001/jamaneurol.2022.1375.

Thomas, B.A., Cuplov, V., Bousse, A., Mendes, A., Thielemans, K., Hutton, B.F., Erlandsson, K., 2016. PETPVC: a toolbox for performing partial volume correction techniques in positron emission tomography. Phys. Med. Biol. 61, 7975–7993. https://doi.org/10.1088/0031-9155/61/22/7975.

Thomas, B.A., Erlandsson, K., Modat, M., Thurfjell, L., Vandenberghe, R., Ourselin, S., Hutton, B.F., 2011. The importance of appropriate partial volume correction for PET quantification in Alzheimer's disease. Eur. J. Nucl. Med. Mol. Imaging 38, 1104–1119. https://doi.org/10.1007/s00259-011-1745-9.

Videen, T.O., Perlmutter, J.S., Mintun, M.A., Raichle, M.E., 1988. Regional correction of positron emission tomography data for the effects of cerebral atrophy. J. Cereb. Blood Flow Metab. 8, 662–670. https://doi.org/10.1038/jcbfm.1988.113.

Weigand, A.J., Maass, A., Eglit, G.L., Bondi, M.W., 2022. What's the cut-point?: a systematic investigation of tau PET thresholding methods. Alzheimers Res. Ther. 14, 49. https://doi.org/10.1186/s13195-022-00986-w.

Yang, J., Huang, S.C., Mega, M., Lin, K.P., Toga, A.W., Small, G.W., Phelps, M.E., 1996. Investigation of partial volume correction methods for brain FDG PET studies. IEEE Trans. Nucl. Sci. 43, 3322–3327. https://doi.org/10.1109/23.552745.

Yoon, B., Guo, T., Provost, K., Korman, D., Ward, T.J., Landau, S.M., Jagust, W.J., 2022. Abnormal tau in amyloid PET negative individuals. Neurobiol. Aging 109, 125–134. https://doi.org/10.1016/j.neurobiolaging.2021.09.019.